

# Novel Functional Polymers: Poly(dimethylsiloxane)-Polyamide Multiblock Copolymer. VII.\* Oxygen Permeability of Aramid-Silicone Membranes in a Gas-Membrane-Liquid System

TAKEO MATSUMOTO,<sup>1,2</sup> TOSHIRO UCHIDA,<sup>1</sup> AKIO KISHIDA,<sup>1</sup> TSUTOMU FURUZONO,<sup>1</sup> IKURO MARUYAMA,<sup>3</sup> MITSURU AKASHI<sup>1</sup>

<sup>1</sup>Department of Applied Chemistry and Chemical Engineering, Faculty of Engineering, Kagoshima University, 1-21-40 Korimoto, Kagoshima 890, Japan;

<sup>2</sup>Tsukuba Research Laboratory, NOF Corporation, 5-10, Tokodai, Tsukuba 300-26, Japan;

<sup>3</sup>Department of Clinical Laboratory Medicine, Faculty of Medicine, Kagoshima University, 8-35-1 Sakuragaoka, Kagoshima 890, Japan

Received 23 July 1996; accepted 24 October 1996

**ABSTRACT:** Poly(dimethylsiloxane) (PDMS) and aromatic polyamide (aramid) multiblock copolymer (PAS) membranes containing  $\geq 55$  wt % of PDMS were prepared. Their tensile strength, morphology, and oxygen permeation property were investigated. The observed high tensile strength of PAS with 55 wt % of PDMS indicates the presence of PDMS-aramid co-continuous phases with lamellar structures; furthermore, the microphase-separated structures of PAS membranes were observed by means of transmission electron microscopy. The overall oxygen permeation resistance of a conventional silicone rubber showed typical dependence on stirrer speed, which was derived from the macroscopic relationship between the membrane-liquid interfacial resistance and the stirrer speed. However, the overall oxygen permeation resistances of the PAS membranes were found not to simply depend on stirrer speed. Combining with the oxygen permeability of PAS in the case of a gas-membrane-gas system, the interface resistances of the membranes were evaluated. The interface resistances of the PAS membranes with the two-phase nature were more susceptible to the hydrodynamic parameter than that of the silicone rubber and became lower than that of the silicone rubber at higher stirrer speeds. The low interface resistance together with the high tensile strength of the PAS membranes enables us to provide highly oxygen permeable membranes in practical applications with a membrane-liquid interface. © 1997 John Wiley & Sons, Inc. *J Appl Polym Sci* **64**: 1153–1159, 1997

**Key words:** poly(dimethylsiloxane); silicone; polyamide; multiblock copolymer; oxygen permeability; interface resistance

\* For Part I, cf. Ref. 13; for Part II, cf. Ref. 17; for Part III, cf. Ref. 14; for Part IV, cf. Ref. 18; for Part V, cf. Ref. 15; for Part VI, cf. Ref. 22.

Correspondence to: M. Akashi.

Contract grant sponsor: Ministry of Education, Science, Sports, and Culture, Japan.

Contract grant number: 07558257.

Contract grant sponsor: Ministry of Health and Welfare, Government of Japan.

© 1997 John Wiley & Sons, Inc. CCC 0021-8995/97/061153-07

## INTRODUCTION

Silicone polymers principally based on poly(dimethylsiloxane) (PDMS) have been widely used in medical fields because of their unique properties such as biocompatibility, chemical inertness, low surface energy, lubricity, flexibility, and gas

permeability.<sup>1-4</sup> When it comes to applications such as artificial lungs<sup>5</sup> and contact lenses,<sup>6,7</sup> high gas permeability and good biocompatibility are among the most desired properties of silicone polymers. Such an application, however, is sometimes limited by the polymers' poor mechanical properties, especially low tensile strength due to the low level of intermolecular forces in the absence of reinforcing fillers. To improve the mechanical properties without sacrificing the desired properties of silicone polymers, many investigations have been reported on the synthesis and characterization of block or segmented siloxane copolymers including PDMS as the soft segment.<sup>8-11</sup> Consideration, however, also needs to be given to both the bulk and the surface properties important to an application in biomedical devices; detailed study on this point was not conducted.

Focusing on the high permeability to many gases and very good biocompatibility, we have been investigating PDMS and aromatic polyamide (aramid) multiblock copolymers, that is, aramid-silicone resins (PAS), first synthesized by Kajiyama et al.<sup>12</sup> In previous articles, we studied the synthesis and characteristics of PAS from a novel biomaterial point of view.<sup>13-18</sup> In that study, PAS exhibited many of the desirable properties of aramid and PDMS for medical applications. The interaction between biomolecules (protein, cell, and tissue) and PAS surfaces was found to be equal or relatively low compared with SILASTIC® 500-1.<sup>15</sup> We have reported that PAS can be molded into many forms, such as films and hollow fibers.<sup>16</sup> Their surface properties were also investigated in detail,<sup>14,17</sup> because the surface properties of copolymers such as PAS, which seem to be strongly influenced by the molding method, play an important role in their functionality, especially in medical applications.

The two-phase nature of PAS caused by the high degree of incompatibility of the PDMS segment with the aramid segment was clarified in part by evaluating the gas permeation and dynamic thermomechanical properties.<sup>18</sup> The gas permeation properties in a gas-membrane-gas system can be well predicted by the PDMS contribution to the continuous phase. The presence of a liquid-membrane interface in most biomedical devices, however, urges us to understand the difference between the gas permeation in the solid phase and that in the liquid phase, together with the effect of boundary layer phenomena. In this study, for the purpose of clarifying the oxygen permeation behavior through PAS membranes to wa-

ter, the oxygen permeability was investigated by means of a gas-membrane-liquid method. We discuss overall resistance to oxygen permeation between two phases, which consists of resistance inherent to the PAS membrane and the liquid-membrane interfacial resistance, varying with hydrodynamic parameters.

## EXPERIMENTAL

### Preparation of PAS and Membranes

PAS was prepared by low-temperature solution polycondensation through a two-step procedure according to the literature.<sup>13</sup> Briefly,  $\alpha,\omega$ -dichloroformyl-terminated aramid oligomers were prepared by the reaction of 3,4'-diaminodiphenyl ether (Wakayama Seika Industry Co., Wakayama, Japan) with a calculated excess of isophthaloyl chloride (Wako Pure Chemical, Osaka, Japan) in a chloroform-triethylamine-hydrochloride system at  $-15^{\circ}\text{C}$  for 5 min in the presence of triethylamine as the hydrogen chloride acceptor under nitrogen. Next, the preformed aramid oligomers were reacted with PDMS-diamine (number-average molecular weight [ $M_n$ ] of 1,680; Shin-Etsu Chemical Co., Tokyo, Japan) at  $-15^{\circ}\text{C}$  for 1 h. The reaction was then continued at room temperature for 48 h under nitrogen. The polymers were isolated by pouring the reaction mixture into methanol; a low-molecular-weight fraction enriched in PDMS was removed by washing the product three times with *n*-hexane; the residue was dried at  $60^{\circ}\text{C}$  for 48 h under vacuum. The observed PDMS contents of PAS in bulk were calculated from the  $\text{SiCH}_3/\text{aromatic H}$  ratio in the  $^1\text{H}$  nuclear magnetic resonance spectra, measured with a JEOL EX-90 (JEOL, Tokyo, Japan). The inherent viscosity of PAS was measured with an Ostwald's viscometer at a concentration of 0.5 g/dL in *N,N'*-dimethylacetamide (DMAc) at  $30^{\circ}\text{C}$ .

PAS membranes were cast from a 5 wt % DMAc solution on a TEFLON® sheet, and then the solvent was evaporated at  $50^{\circ}\text{C}$  for 5 days. Finally, the membranes were dried at  $60^{\circ}\text{C}$  for 24 h *in vacuo*, and PAS membranes ranging in thickness from 30 to 100  $\mu\text{m}$  were obtained. A SILASTIC® 500-1 membrane with thickness of 125  $\mu\text{m}$  was kindly donated by Dow Corning Japan Co. (Tokyo, Japan).

### Tensile Strength Measurement

Tensile strength was determined by the stress-strain curves obtained with Autograph® AGS-

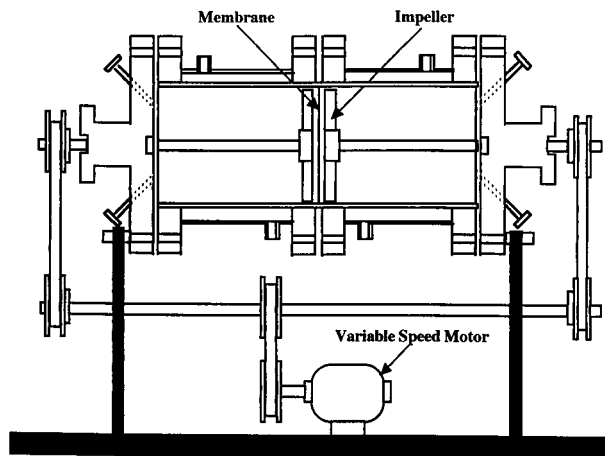


**Figure 1** Experimental apparatus for oxygen permeability measurement.

5kNB (Shimazu Co., Kyoto, Japan) at an elongation rate of 1.0 mm/min. Measurements were performed at room temperature with membrane specimens (3 mm wide, 15 mm long, and 0.1 mm thick), and three individual determinations were averaged.

#### Transmission Electron Microscopy

The ultrathin PAS specimens were cast from a 0.5 wt % DMAc solution on carbon-coated copper electron microscope grids of large mesh size (400 mesh per inch). The specimens were stained with a vapor of  $\text{RuO}_4$  for 15–20 min. Transmission electron microscopy (TEM) was done with a Hitachi H-7000 transmission electron microscope (Hitachi Ltd., Tokyo, Japan) at 80 kV accelerating voltage.

#### Oxygen Permeability Measurement

The equipment used for the oxygen permeation experiment was fabricated by ourselves, referring to that of Okazaki and Yoshida.<sup>20</sup> A picture of the equipment is shown in Figure 1. This apparatus is able to apply to the permeation experiment of liquid-to-liquid, liquid-to-gas, and gas-to-liquid system. Both of the asymmetric inner cylindrical tanks are made of poly(methyl methacrylate) of 50 mm inner diameter and 60 mm length, and the other parts are made of polyvinyl chloride (PVC). The sample membrane is placed between the two tanks with a PVC spacer of 5-mm thickness. The impeller installed in the tanks has six wings of 10-mm width and 45-mm diameter. The rotation speed is altered by changing the applied voltage.

For the gas permeation measurement, phosphate-buffered saline (PBS) is filled in the right-hand tank under stirring and oxygen gas is purged into the empty left-hand tank without stirring. Thus, oxygen can permeate from left to right through the membrane. The oxygen dissolved in PBS through the membrane permeation is measured with an automatic blood gas analyzer, AVL-30 (Radiometer Medical A/S, Copenhagen, Denmark).

## RESULTS AND DISCUSSION

#### Tensile Strength

PAS and the PAS membranes prepared are summarized in Table I. The stress-strain curves of the PAS membranes are shown in Figure 2. The tensile properties of the membranes are highly dependent on the PDMS content in the block copolymers, and the tensile strength of PAS was significantly higher than that of SILASTIC® 500-1. The higher tensile strength of the PAS membranes compared with SILASTIC® 500-1 indicates that PAS with 55 wt % of PDMS has as a high structural regularity as PDMS-aramid co-continuous phases in lamella. The high ultimate elongation of PAS with 70 wt % of PDMS implies that the PDMS phase exists as the continuous phase with the aramid phase present as discrete domains.<sup>21</sup> The elongation at break of PAS with 55 wt % of PDMS was coincident with that of the aramid homopolymer.

#### Morphology

The transmission electron micrographs of ultrathin membranes (ca. 50 ~ 80 nm thickness) of PAS are shown in Figure 3. We confirmed that the PDMS component was more easily stained with  $\text{RuO}_4$  than was the aramid component.<sup>22</sup> Thus, the black area indicates a PDMS phase, and the white area corresponds to an aramid phase. Two-phase morphology was clearly observed for the PAS membranes with 55 and 70 wt % of PDMS, despite enrichment of the PDMS segment on the outermost surface of the PAS membranes, revealed by the X-ray photoelectron spectroscopy and dynamic contact angle measurements.<sup>14,17</sup>

#### Oxygen Permeability

A schematic view of a cross-section of the membrane is shown in Figure 4. The buildup of oxygen

**Table I** Preparation of PAS and PAS Membranes

PAS	$M_n$		PDMS Content <sup>a</sup> (wt %)	$\eta_{inh}^b$ (dL/g)	Thickness ( $\mu\text{m}$ )
	PDMS	Aramid <sup>a</sup>			
PAS-55	1,680	1,375	55	0.51	
PAS-55-90	1,680	1,375	55		90
PAS-70	1,680	720	70	0.27	
PAS-70-30	1,680	720	70		30
PAS-70-60	1,680	720	70		60

<sup>a</sup> Calculated from Si-CH<sub>3</sub>/aromatic-H ratio in the <sup>1</sup>H nuclear magnetic resonance spectrum.

<sup>b</sup> Measured at a concentration of 0.5 g/dL in DMAc at 30°C.

partial pressure,  $\Gamma$  in mmHg, was recorded as a function of time. From the material balance,

$$V d\Gamma/dt = KA(\Gamma^* - \Gamma) \quad (1)$$

where  $V$  is the buffer solution volume (cm<sup>3</sup>),  $A$  is the membrane surface area (cm<sup>2</sup>),  $\Gamma$  is the partial pressure of oxygen in buffer solution,  $\Gamma^*$  is the equilibrated partial pressure of oxygen in the gas phase, and  $K$  is the overall oxygen permeation coefficient (cm/sec).<sup>23</sup> Integrating eq. (1) from time (sec)  $t = 0$  to  $t = T$ , one obtains

$$\log([\Gamma^* - \Gamma_0]/[\Gamma^* - \Gamma]) = (KA/2.303V)t \quad (2)$$

The overall oxygen permeation resistance,  $1/K$ , of the PAS membranes can be easily calculated

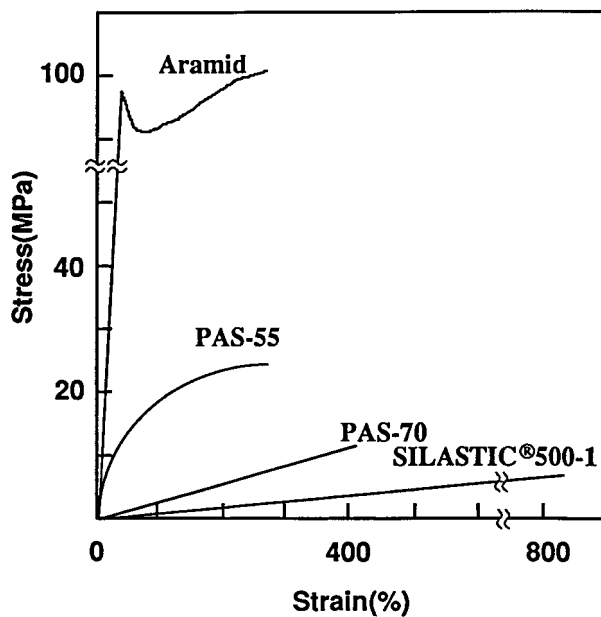


**Figure 2** Stress-strain curves for PAS and SILASTIC® 500-1.

from the slope of semilogarithmic plots of eq. (2), assuming the existence of a quasi-steady-state regime—neglecting the rate of oxygen accumulation in the membrane phase.<sup>24</sup>

Figure 5 shows the overall oxygen permeation resistances ( $1/K$ ) of the membranes at the various stirrer speeds ranging from 80 to 580 rpm.  $1/K$

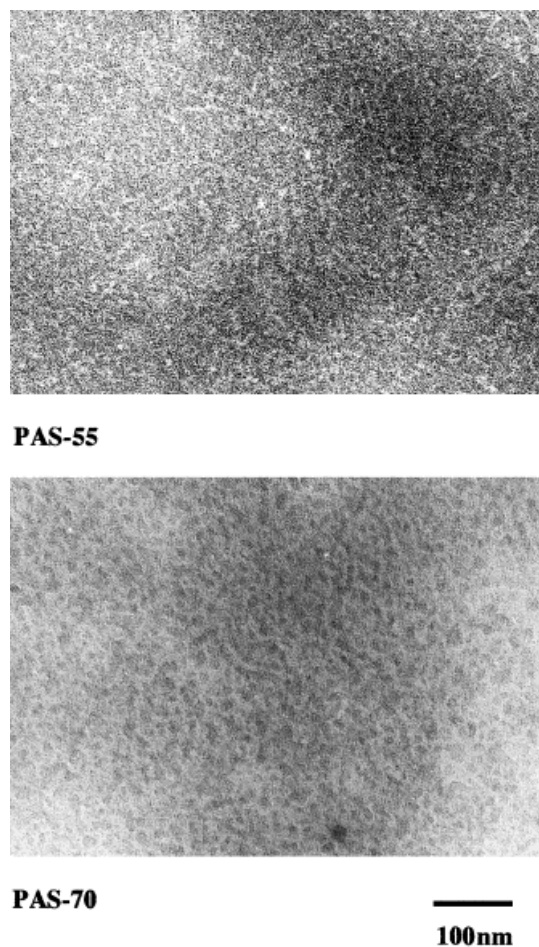


**Figure 3** Transmission electron micrographs of the membrane.

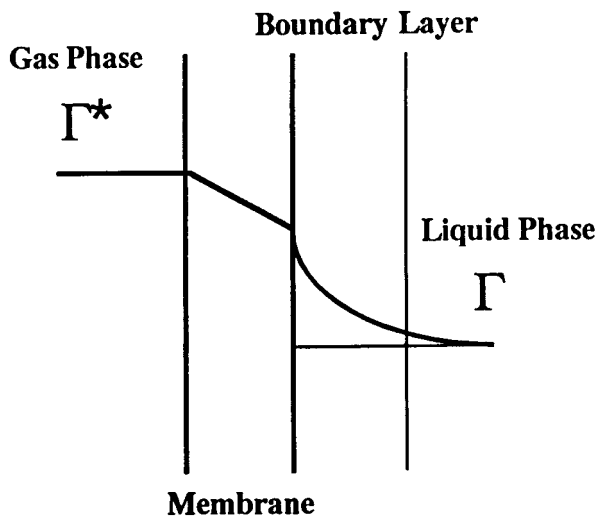


Figure 4 A schematic view of a cross-section of the membrane.

decreased exponentially with increasing the stirrer speeds. The overall oxygen permeation resistance in terms of permeation coefficients is broken down into two resistances inherent to its component membrane and liquid-membrane interface in series:<sup>25</sup>

$$1/K = 1/K_m + 1/K_L \quad (3)$$

where  $K_m$  is the membrane permeation coefficient (cm/sec), and  $K_L$  is the liquid-membrane interfacial permeation coefficient (cm/sec). The liquid-membrane interface resistance ( $1/K_L$ ) was assumed to be inversely proportional to the stirrer speed,  $n$  (rpm), raised to some exponent,  $c$ , esti-

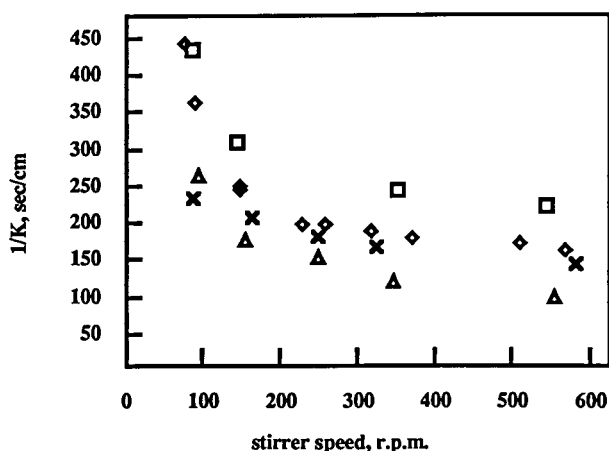


Figure 5 Overall oxygen permeation resistances of the membranes at the various stirrer speeds. (○) PAS-55-90, (△) PAS-70-30, (◇) PAS-70-60, (X) SILASTIC® 500-1.

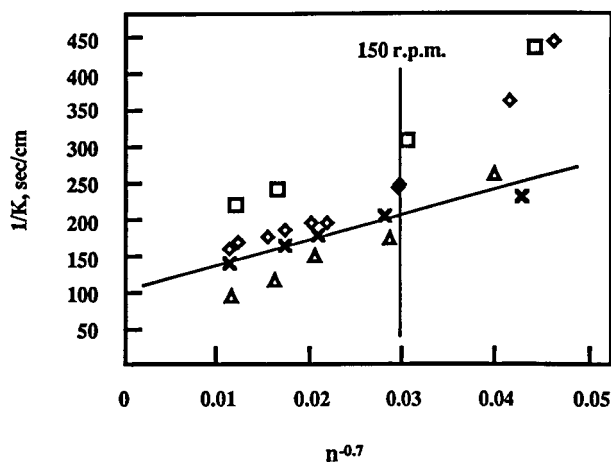


Figure 6 Overall oxygen permeation resistances of the membranes as a function of  $n^{-0.7}$ .  $n$  is the stirrer speed expressed in rpm. (○) PAS-55-90, (△) PAS-70-30, (◇) PAS-70-60, (X) SILASTIC® 500-1.

imating the macroscopic relationship between interfacial resistance and Reynolds number ( $Re$ ;  $\omega r^2 v$ , where  $\omega$  is the angular velocity [rad/sec],  $r$  is the membrane radius [cm], and  $v$  is the kinematic viscosity [ $\text{cm}^2/\text{sec}$ ]), the stirrer speed.<sup>25</sup> Therefore, the membrane resistance may be determined if the overall resistances, plotted as a function of  $(1/n)^c$ , are extrapolated with a best statistical fit straight line to infinite stirrer speed.

In Figure 6, the overall oxygen permeation resistances of the membranes are plotted by setting  $c$  equal to 0.7, which was reported to yield the best statistical fit in many types of interfacial transport data.<sup>26-28</sup> The plot for the silicone membrane, SILASTIC® 500-1, gave a straight line over the wide range of speeds used, and its membrane resistance obtained by extrapolation was almost the same as reported in the literature.<sup>20</sup> On the other hand, data obtained for the PAS membranes did not show excellent agreement with theoretical predictions based on a stagnant boundary layer formation; there seem to be critical stirrer speeds around 150 rpm separating two regimens of the stirrer speed. The overall oxygen permeation resistances of the PAS membranes containing 70 wt % of PDMS were equal to or less than that of the conventional silicone rubber at stirrer speeds  $\geq 150$  rpm.

The modified Wilson plot described above implicitly assumes that a unique exponent yielding a straight line does exist over the entire range of speeds or, in effect, that the flow regimen of the boundary layer formed on the membrane is the same for all speeds. The plots obtained for the PAS membranes, however, showed two distinct

regions; therefore, the true membrane resistance may not be determined by extrapolating  $1/K$  to infinite stirrer speed.

Eq. (3) can be rewritten as follows:<sup>23,24</sup>

$$1/K = SL/P + 1/K_L \quad (4)$$

where  $P$  is the oxygen permeability of the membrane ( $\text{cm}^3$  standard temperature and pressure [STP]  $\text{cm}/\text{cm}^2$  sec  $\text{cmHg}$ )  $S$  is the solubility of oxygen in water ( $\text{cm}$  [STP]/ $\text{cm}^3$   $\text{cmHg}$ ), and  $L$  is the thickness of the membrane ( $\text{cm}$ ). Because the transport mechanism of oxygen through the membrane in liquid-membrane-gas permeation is assumed to be about the same as in the case of gas-membrane-gas permeation,<sup>24</sup>  $P$  can be determined by a routine high-vacuum method.<sup>25</sup> The two-phase nature of the PAS membranes, similar to that obtained in the previous study,<sup>18</sup> on which the gas permeability of the membrane mainly depended, was confirmed in part by both the tensile strength properties and TEM. Therefore, the oxygen permeability of PAS membranes with 55 and 70 wt % of PDMS may be determined as  $1.8 \times 10^{-8}$  and  $2.1 \times 10^{-8}$  ( $\text{cm}^3$  [STP]  $\text{cm}/\text{cm}^2$  sec  $\text{cmHg}$ ), respectively, from the previous prediction.<sup>18</sup> The oxygen permeability of SILASTIC® 500-1 is reported as  $6 \times 10^{-8}$  ( $\text{cm}^3$  [STP]  $\text{cm}/\text{cm}^2$  sec  $\text{cmHg}$ ).<sup>23</sup> The membrane resistance,  $SL/P$ , was calculated by an  $S$  of  $3.7 \times 10^{-4}$  ( $\text{cm}^3$  [STP]/ $\text{cm}^3$   $\text{cmHg}$ ) at 25°C. Subtraction of the calculated membrane resistance from the measured overall oxygen permeation resistance yields the interface resistance.

The liquid-membrane interface resistances are plotted as a function of  $n^{-0.7}$  in Figure 7. The interface resistances of the PAS membranes decreased with increasing stirrer speeds having two distinct regions, but were not dependent on the membrane thickness. All of the interface resistances of the PAS membranes had almost the same dependence on the stirrer speed; at a stirrer speed  $< 150$  rpm, the interface resistances of the PAS membranes were higher than that of the silicone rubber, and at stirrer speeds  $\geq 150$  rpm, they were lower than that of the silicone rubber, while the interface resistance of the silicone rubber showed a linear relationship with  $n^{-0.7}$ . It was indicated by measurement of the torque on a cellophane membrane with  $Re$  characterizing the turbulence in the bulk of the liquid that: above  $Re \approx 30,000$ , corresponding to a stirrer speed of about 320 rpm, the membrane boundary layer is turbulent; below  $Re \approx 20,000$ , a stirrer speed of about 210 rpm, the boundary layer is laminar. A transition region,

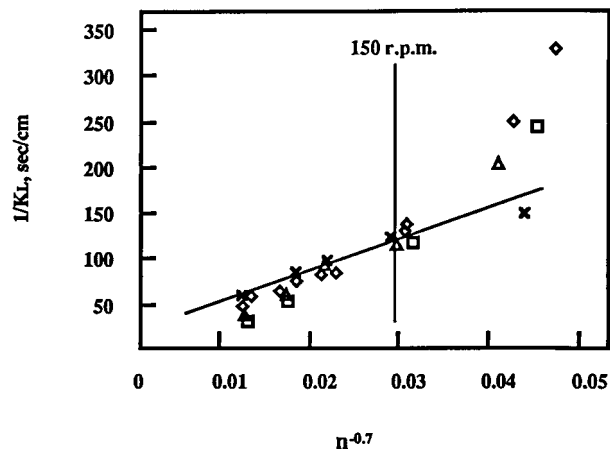


**Figure 7** Liquid-membrane resistances as a function of  $n^{-0.7}$ .  $n$  is the stirrer speed expressed in rpm. (○) PAS-55-90, (△) PAS-70-30, (◇) PAS-70-60, (X) SILASTIC® 500-1.

where the flow changes from laminar to turbulent, may exist beginning at  $Re \approx 20,000$ – $25,000$ .<sup>26</sup> It is assumed that the dependence of the flow regimen in the proximity of the PAS membranes on the stirrer speed is similar to that of the cellophane membrane rather than the silicone rubber; in other words, the interface resistances of the PAS membranes with the two-phase nature are more susceptible to the hydrodynamic parameter relevant to the stirrer speed than that of the silicone rubber.

## CONCLUSIONS

The oxygen permeation properties of PAS membranes in the gas-membrane-liquid system were clarified in part by evaluating the interface resistances of the membranes. The interface resistances of the PAS membranes with the two-phase nature were more susceptible to the hydrodynamic parameter than that of the silicone rubber and became lower than that of the silicone rubber at higher stirrer speeds. The low interface resistance together with the high tensile strength of the PAS membranes enables us to provide highly oxygen permeable membranes in practical applications with a membrane-liquid interface.

The authors express their thanks to Kozo Shiraishi, the president of Shiraishi Hospital and Prof. Yoshito Ikada, Research Center for Biomedical Engineering, Kyoto University, for his assistance in the measuring of oxygen permeability.

## REFERENCES

1. W. Lynch, in *Handbook of Silicone Rubber Fabrication*, Van Nostrand Reinhold Company, New York, 1978.
2. R. Rudolph, J. Abraham, T. Vechione, S. Guber, and M. Woodward, *Plast. Reconstr. Surg.*, **62**, 185 (1978).
3. L. C. Hartman, R. W. Bessette, R. E. Baier, A. E. Meyer, and J. Wirth, *J. Biomed. Mater. Res.*, **22**, 475 (1988).
4. E. E. Frisch, in *Silicones in Artificial Organs*, C. G. Gebelein, Ed., ACS Symposium Series, 1984, Vol. 256, p. 63.
5. J. Kamo, T. Kamata, and T. Takemura, *Jpn. J. Artif. Organs*, **18**, 13 (1989).
6. E. Travnicek, U.S. Pat. 3,996,189 (1976).
7. V. Migonney, M. D. Lacroix, B. D. Ratner, and M. Jozefowicz, *J. Biomater. Sci. Polym. Ed.*, **7**, 265 (1995).
8. L. M. Robeson, A. Noshay, M. Matzner, and C. N. Merriam, *Angew. Makromol. Chem.*, **29/30**, 47 (1973).
9. R. J. Zdrahala, E. M. Firer, and J. F. Fellers, *J. Polym. Sci. Polym. Chem. Ed.*, **15**, 689 (1977).
10. I. Yilgor, A. K. Shaaban, W. P. Steckle, D. Tyagi, G. L. Wilkens, and J. E. McGrath, *Polymer*, **25**, 1800 (1984).
11. D. Tyagi, I. Yilgor, J. E. McGrath, and G. L. Wilkens, *Polymer*, **25**, 1807 (1984).
12. M. Kajiyama, M. Kakimoto, and Y. Imai, *Macromolecules*, **22**, 4143 (1989).
13. T. Furuzono, E. Yashima, A. Kishida, I. Maruyama, T. Matsumoto, and M. Akashi, *J. Biomater. Sci., Polym. Ed.*, **5**, 89 (1993).
14. T. Furuzono, K. Seki, A. Kishida, T. Ohshige, K. Waki, I. Maruyama, and M. Akashi, *J. Appl. Polym. Sci.*, **59**, 1059 (1996).
15. T. Furuzono, A. Kishida, M. Yanagi, T. Matsumoto, T. Kanda, T. Nakamura, T. Aiko, I. Maruyama, and M. Akashi, *J. Biomater. Sci., Polym. Ed.*, **7**, 870 (1996).
16. T. Furuzono, A. Kishida, M. Akashi, I. Maruyama, T. Miyazaki, Y. Koinuma, and T. Matsumoto, *Jpn. J. Artif. Organs*, **22**, 370 (1993).
17. A. Kishida, T. Furuzono, T. Ohshige, I. Maruyama, T. Matsumoto, H. Itoh, M. Murakami, and M. Akashi, *Angew. Makromol. Chem.*, **220**, 89 (1994).
18. T. Matsumoto, Y. Koinuma, K. Waki, A. Kishida, T. Furuzono, I. Maruyama, and M. Akashi, *J. Appl. Polym. Sci.*, **59**, 1067 (1996).
19. J. S. Trent, J. I. Scheinbeim, and P. R. Couchman, *Macromolecules*, **16**, 589 (1983).
20. M. Okazaki and F. Yoshida, *Kobunshi Ronbunshu*, **34**, 255 (1977).
21. Y. Imai, M. Kajiyama, S. Ogata, and M. Kakimoto, *Polym. J.*, **17**, 1173 (1985).
22. T. Furuzono, K. Senshu, A. Kishida, T. Matsumoto, and M. Akashi, *Polym. J.*, **29**, 201 (1997).
23. S. Hwang, T. Tang, and K. Kammermeyer, *J. Macromol. Sci. Phys.*, **B5**, 1 (1971).
24. L. Nicodemo, F. Bellucci, R. Le Rose, and C. Carfagna, *J. Membr. Sci.*, **43**, 177 (1989).
25. Y. Tsujita, K. Yoshimura, H. Yoshimizu, A. Takizawa, and T. Kinoshita, *Polymer*, **34**, 2597 (1993).
26. K. A. Smith, C. K. Colton, E. W. Merrill, and L. B. Evans, *Chem. Eng. Prog. Sym. Ser.*, **64**, 45 (1968).
27. T. G. Kaufmann and E. F. Leonard, *AIChE J.*, **14**, 421 (1968).
28. J. Marangozis and A. I. Johnson, *Can. J. Chem. Eng.*, **40**, 231 (1962).